

Entanglement, soft modes, and celestial holography

Hong Zhe Chen^{1,2}, Robert Myers,¹ and Ana-Maria Raclariu^{1,3}

¹*Perimeter Institute for Theoretical Physics, 31 Caroline Street North, Waterloo N2L 2Y5, Canada*

²*Department of Physics and Astronomy, University of Waterloo, Waterloo, Ontario N2L 3G1, Canada*

³*Institute for Theoretical Physics, University of Amsterdam, Science Park 904, Postbus 94485, 1090 GL Amsterdam, The Netherlands*



(Received 10 October 2023; accepted 8 May 2024; published 14 June 2024)

We evaluate the vacuum entanglement entropy across a cut of future null infinity for free Maxwell theory in four-dimensional Minkowski spacetime. The Weyl invariance of 4D Maxwell theory allows us to embed the Minkowski spacetime inside the Einstein static universe. The Minkowski vacuum can then be described as a thermofield double state on the (future) Milne wedges of the original and inverted Minkowski patches. We show that the soft mode contribution to entanglement entropy is due to correlations between asymptotic charges of these Milne wedges or, equivalently, nontrivial conformally soft (or edge) mode configurations at the entangling surface.

DOI: 10.1103/PhysRevD.109.L121702

Introduction. Entanglement is a distinguishing feature of quantum physics, shaping many properties of complex interacting systems. The entanglement between any subsystem R and its complement can be quantified by the entanglement entropy,

$$S_{\text{vN}}(R\rho) = -\text{tr}(R\rho \log R\rho), \quad (1)$$

i.e., the von Neumann entropy of the reduced density matrix $R\rho$ describing the state on R . Remarkably, the AdS/CFT correspondence [1] equates the entanglement entropy of subregions in the boundary conformal field theory (CFT) with a generalized gravitational entropy in the anti-de Sitter (AdS) bulk [2–6]. This discovery has sparked many exciting advances in our understanding of quantum gravity using the tools of quantum information, including connections to quantum error correction [7,8] and insights into the black hole information paradox [9–11].

Concurrently, gauge and gravity theories in asymptotically flat spacetimes were shown to have a very rich infrared structure [12–15]. Here, the vacuum is infinitely degenerate, with different vacua related by asymptotic symmetries or, equivalently, the addition of soft particles [14–17]. Arising from these developments, celestial holography, e.g., [18–20], proposes a duality between a $(3+1)$ -dimensional asymptotically flat spacetime and a two-dimensional celestial CFT (CCFT). Entanglement and

the representation of bulk subregions in the new holographic framework have been unexplored so far.

In this Letter, we take essential steps in formulating a new entry in the flat space holographic dictionary relating bulk subregions in 4D Minkowski spacetime and observables in 2D celestial CFT. It was noted in [21] that infrared effects may contribute nontrivially to the entanglement entropy across a cut on future null infinity \mathcal{I}^+ . Pursuing this direction further, we examine the vacuum entanglement across a cut on \mathcal{I}^+ for free Maxwell theory in four-dimensional Minkowski spacetime. This entangling surface on \mathcal{I}^+ is defined by the future light cone emanating from a point in the Minkowski geometry. Following standard convention, we refer to the spacetime region to the future of this light cone as the future Milne patch—see Fig. 1(a). Hence, we are considering the entanglement entropy (1) for the mixed state on this region.

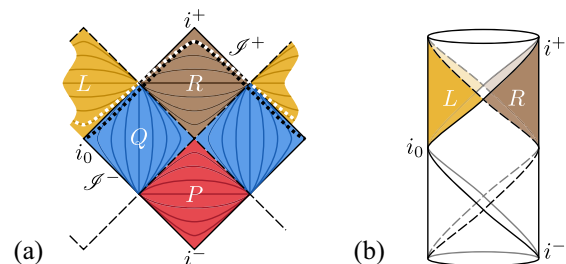


FIG. 1. (a) Penrose diagram of Minkowski spacetime and associated inverted spacetime (delineated by solid and dashed diagonal lines, respectively). They overlap in the patch Q , while P , R , L denote Milne patches. Minkowski (black) and Milne (white) Cauchy slices near \mathcal{I}^+ are drawn as dashed curves. (b) Conformal image in the Einstein universe.

Published by the American Physical Society under the terms of the [Creative Commons Attribution 4.0 International license](https://creativecommons.org/licenses/by/4.0/). Further distribution of this work must maintain attribution to the author(s) and the published article's title, journal citation, and DOI. Funded by SCOAP³.

To this end, we leverage the Weyl invariance of 4D Maxwell theory to embed the Minkowski spacetime inside the Einstein static universe $\mathbb{R} \times S^3$. In this context, a full Cauchy slice is formed by Cauchy slices for Milne wedges of the original geometry (R) and its counterpart (L) in the “inverted” Minkowski geometry produced with a conformal inversion of the original spacetime—see Fig. 1. We will show that the mixed state ${}^R\rho$ can be purified as a thermofield double state on L and R . Along the way, we develop new methods to characterize conformal primary sectors of bulk subregions. A challenge in studying this entanglement is then the treatment of soft modes. We attribute the associated entanglement to asymptotic charge fluctuations and explain how spacetime entanglement could arise holographically from the celestial CFT. Due to the universality of soft physics, we expect similar methods to be useful to describe the asymptotic physics of spacetime fluctuations in (quantum) gravity [22–24].

Preliminaries. A key step in celestial holography is replacing plane waves by boost eigenfunctions, transforming as conformal primaries under the Lorentz group [25]. These conformal primary wave functions (CPWs) in free Maxwell theory in $(3+1)$ -dimensional Minkowski spacetime, with coordinates X , are

$$A_{a;\mu}^{\Delta,\pm}(\mathbf{w}; X) = \frac{m_{a;\mu}^{\pm}(\mathbf{w}; X)}{[-\hat{q}(\mathbf{w}) \cdot X_{\pm}]^{\Delta}}, \quad X_{\pm}^{\mu} = X^{\mu} \mp i\epsilon \hat{n}^{\mu}, \quad (2)$$

labeled by points \mathbf{w} in celestial space, corresponding to a section of \mathcal{I}^{\pm} reached by null rays $\pm\hat{q}(\mathbf{w})$. The $m_{a;\mu}^{\pm}$ label photon polarizations, but their precise form will be unimportant in the following [26,27]. With \hat{n} obeying $\hat{n} \cdot \hat{q}(\mathbf{w}) = 1$, the $i\epsilon$ provides a prescription to cross the $\hat{q} \cdot X = 0$ surface.

The modes (2) have eigenvalues Δ under boosts toward $\hat{q}(\mathbf{w})$, dual to dilations about \mathbf{w} in celestial space. These $+/-$ modes form a basis of solutions with positive/negative-definite frequencies with respect to Minkowski time, provided $\Delta = 1 + i\lambda, \lambda \in \mathbb{R}$. Here, λ is also a frequency with respect to Milne time τ ,

$$\partial_{\tau} A_a^{1+i\lambda} \stackrel{\epsilon}{=} -i\lambda A_a^{1+i\lambda}, \quad \tau = \frac{1}{2} \log(-X^2), \quad (3)$$

where $\stackrel{\epsilon}{=}$ denotes equality when $\epsilon \rightarrow 0$. The $\Delta = 1$ ($\lambda = 0$) modes yield the Goldstone wave functions $A_a^G(\mathbf{w}, X)$, while their canonically conjugate conformally soft partners $A_a^{\text{CS}}(\mathbf{w}, X)$ (which also have $\Delta = 1$) were constructed in [28]—see also Supplemental Material [27].

The asymptotic symmetries of pure Maxwell theory are generated by asymptotic charges [15,29]

$$Q[\alpha] = \int_{\mathcal{I}_{\mp}^{\pm}} \alpha * F \hat{=} \int_{\mathcal{I}^{\pm}} d\alpha \wedge *F, \quad (4)$$

where \mathcal{I}_{\mp}^{\pm} (\mathcal{I}_{\pm}^{\mp}) is the past (future) boundary of \mathcal{I}^+ (\mathcal{I}^-) and the last equality holds on shell. Turning on A^{CS} changes the values of the charges (4). In contrast, the global charge obtained with constant α vanishes in free Maxwell theory.

From CPWs, one constructs operators

$$\mathcal{O}_a^{\Delta,\pm}(\mathbf{w}) = -i \langle A_a^{\Delta,\pm}(\mathbf{w}), A \rangle = \mathcal{O}_a^{\Delta,*\mp}(\mathbf{w})^{\dagger}. \quad (5)$$

Here $\langle \cdot, \cdot \rangle$ denotes the spacetime inner product among spin-1 conformal primary wave functions [28]. Replacing A^{Δ} by A^G, A^{CS} moreover defines the (conformally) soft operators $\mathcal{Q}_a(\mathbf{w}) = Q[\alpha^G], \mathcal{S}_a(\mathbf{w})$, respectively. These can be regarded as operators in the CCFT, exciting CPWs in the Minkowski bulk with S -matrix elements encoded by CCFT correlation functions.

Beyond the Minkowski patch. To prepare our entanglement calculations, we employ the Weyl invariance of 4D Maxwell theory to extend the CPWs (2) beyond the Minkowski patch. We first consider an inverted Minkowski patch covered by coordinates \underline{X}^{μ} —see Fig. 1. In the overlap $\underline{X}^2, X^2 > 0$ with the original Minkowski patch, an inversion $\underline{X}^{\mu} = \frac{X^{\mu}}{X^2}$ and Weyl transformation relate the two geometries. Given the Weyl invariance of the 4D Maxwell theory, the gauge field \underline{A} in the inverted patch is simply related to the original A by

$$\underline{A}_{\mu}(\underline{X}) = \frac{\partial X^{\nu}}{\partial \underline{X}^{\mu}} A_{\nu}(X), \quad X^2 > 0. \quad (6)$$

The inverted CPWs (2) are found to be proportional to shadow wave functions

$$\underline{A}_{a;\mu}^{\Delta,\pm}(\mathbf{w}; \underline{X}) \stackrel{\epsilon}{=} e^{\pm i\pi(\Delta-1)} \tilde{A}_{a;\mu}^{\Delta,\pm}(\mathbf{w}; \underline{X}). \quad (7)$$

The shadow wave functions $\tilde{A}_a^{\Delta,\pm}$ [25] yield an alternate set of CPWs. We review their defining properties in [27]. The $\epsilon \rightarrow 0$ limit above ensures Eq. (7) crosses $\hat{q} \cdot X = 0 = \hat{q} \cdot \underline{X}$ in the overlap region consistently with the original mode (2). While Eq. (6) only applies in the overlap of the two Minkowski patches, the result (7) evolves to a solution over the full inverted patch.

Note that inversions and shadow transforms preserve the space of solutions and, moreover, both \underline{A}^{Δ} and \tilde{A}^{Δ} have opposite Milne frequency with respect to A^{Δ} . Therefore, a proportionality (7) between the former modes is unsurprising. We expect a similar relation between shadows and inversions to be a general property of Weyl-invariant theories—see also [30,31].

Complementary Milne patches. The two Minkowski spacetimes are also conformally mapped to the Einstein universe $\mathbb{R} \times S^3$ as in Fig. 1(b) [32]. The future null Minkowski boundary \mathcal{I}^+ (plus i_0) is a Cauchy surface for the Einstein universe. Another Cauchy surface is given by the union of the Cauchy surfaces for the (future) Milne patches of the

original and inverted Minkowski patches, plus the surface (on \mathcal{I}^+) between them. We denote these Milne patches as left (L) and right (R), respectively. Hence, a state on \mathcal{I}^+ should admit a decomposition in terms of L, R states, as illustrated in Fig. 1. This will allow us to evaluate the entanglement across the cut on \mathcal{I}^+ connecting the L, R patches.

We proceed by constructing CPWs associated with the Milne patches. The modes (2) can be decomposed into ${}^L\tilde{A}^\Delta, {}^R A^\Delta$ with initial data supported, respectively, on L and R Cauchy surfaces

$$A^{\Delta,\pm} \stackrel{\epsilon}{=} e^{\pm i\pi(\Delta-1)} {}^L\tilde{A}^\Delta + {}^R A^\Delta, \quad \Delta \notin \mathbb{Z}. \quad (8)$$

Here, $A^{\Delta,\pm}$ agrees with ${}^R A^\Delta$ inside R , and with $e^{\pm i\pi(\Delta-1)} {}^L\tilde{A}^\Delta$ inside L , upon extending Eq. (7) to the full inverted Minkowski patch. Hence, for the principal series (i.e., $\Delta = 1 + i\lambda$, $\lambda \in \mathbb{R}$), the nonsoft (i.e., $\lambda \neq 0$) modes ${}^L\tilde{A}^\Delta, {}^R A^\Delta$ are defined by Eq. (8).

An alternate definition of the L, R modes retains the ϵ regulator to make Eq. (8) an exact equality. Then ${}^L\tilde{A}^\Delta$ and ${}^R A^\Delta$ are smooth finite energy solutions. For instance, their Minkowski inner products can be evaluated using the standard inner products among Minkowski CPWs [25,33]—see also Supplemental Material [27]. Since \mathcal{I}^+ is a Minkowski Cauchy surface and splits into complementary L and R Cauchy surfaces, the inner product decomposes as

$$\langle \cdot, \cdot \rangle \stackrel{\epsilon}{=} {}^L\langle \cdot, \cdot \rangle + {}^R\langle \cdot, \cdot \rangle. \quad (9)$$

Thus, the Minkowski inner products of ${}^L\tilde{A}^\Delta$ and ${}^R A^\Delta$ yield inner products ${}^L\langle \cdot, \cdot \rangle, {}^R\langle \cdot, \cdot \rangle$ in the Milne theories.

Conformally soft modes revisited. Here, we reveal A^{CS} as configurations sourced by charged particles in the Einstein universe beyond the original Minkowski patch.

While A^G has vanishing field strength, A^{CS} possesses electric fields localized on the $\hat{q} \cdot X = 0$ plane and the $X^2 = 0$ light cone. An expansion near \mathcal{I}^\pm reveals that the former leads to a nontrivial electric field F_{ru} near i^0 “sourced” by the radiative modes F_{uz} [34]. Hence, turning on A^{CS} yields a nontrivial asymptotic charge (4)

$$Q^\pm[\alpha, A^{\text{CS}}] = 4\pi d\alpha. \quad (10)$$

To understand this better, we introduce

$$A^{\text{CSI}}(\mathbf{w}_1, \mathbf{w}_2; X) \equiv \int_{\mathbf{w}_1}^{\mathbf{w}_2} A^{\text{CS}}(\mathbf{w}; X) \quad (11)$$

(which is path independent, because A^{CS} is exact on celestial space). The field strength of A^{CSI} is supported on three shock waves: Two planar shock waves along $\hat{q}_1 \cdot X = 0$ and $\hat{q}_2 \cdot X = 0$ carry electric field lines in from infinity, which then transfer to a spherical shock wave at $X^2 = 0$.

Figure 2(a) draws the shock waves of A^{CSI} in the Einstein universe, where a new interpretation of the charges (10)

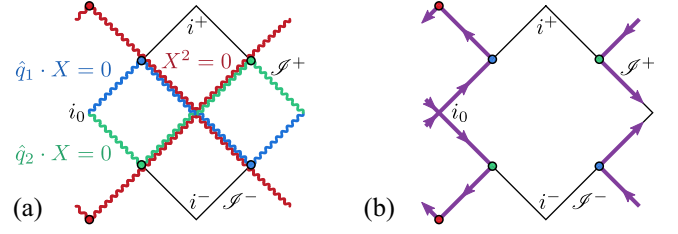


FIG. 2. (a) Shock waves of A^{CSI} extended beyond the Minkowski patch. (b) Charged particles sourcing the shock waves.

emerges. From this perspective, the same field configuration arises as the Lienard-Wiechert fields of two oppositely charged particles, as shown in Fig. 2(b). Moreover, their trajectories contain kinks that act as sources and sinks for the shock waves. We emphasize that the shock waves propagate in the original Minkowski patch, but the charges sourcing them do not. Still, the effect of these charges manifests quite physically in the Minkowski theory, giving precisely [35] the asymptotic charges (4) as a mathematical distribution $\alpha \mapsto Q^\pm[\alpha]$. For example, Eq. (10) matches the dipole source of A^{CS} in Eq. (11).

Soft modes in Milne patches. By analogy with A^G, A^{CS} , we expect pairs of canonically conjugate soft ($\Delta = 1$) modes supported in the L and R patches. As we show in [36], simply taking the $\Delta \rightarrow 1$ limit of ${}^L\tilde{A}^\Delta, {}^R A^\Delta$ violates matching conditions at i^0 [13,37].

A decomposition respecting the matching conditions can be found by considering the extension of A^G, A^{CS} outside the Minkowski patch discussed above, with charges running in between L, R ,

$$A^G = {}^L A^G + {}^R A^G, \quad A^{\text{CS}} = {}^L A^G + {}^L A^E + {}^R A^E. \quad (12)$$

Here, we have introduced the “edge” modes ${}^L A^E, {}^R A^E$ which are localized to an ϵ -regulated shock wave as shown in Fig. 3 and ensure smoothness of A^{CS} in Eq. (12) at finite ϵ . As $\epsilon \rightarrow 0$, the shock wave retreats from the Milne patches, leaving

$${}^L A^G = \lim_{\epsilon \rightarrow 0} A^{\text{CS}}, \quad {}^R A^G = \lim_{\epsilon \rightarrow 0} (A^G - A^{\text{CS}}), \quad (13)$$

which are pure gauge in their respective Milne interiors.

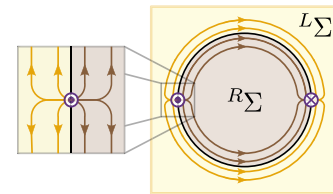


FIG. 3. Electric fields of edge modes ${}^R A^{\text{EI}}$ (brown) and ${}^L A^{\text{EI}}$ (yellow) are part of the ϵ -regulated $X^2 = 0$ shock wave of A^{CSI} . Side panel shows how the shock wave contributes to the normal component of the electric field at $\partial^L\Sigma$ and $\partial^R\Sigma$.

Equation (9) implies that these L, R Goldstone and edge modes are canonically conjugate. Note that only two independent combinations of the four soft modes are permitted in the Minkowski theory, namely A^{CS} and A^{G} .

The Goldstone and edge modes augment the phase space of, e.g., the R Milne patch with soft degrees of freedom ${}^R Q, {}^R S$ defined by the inner product of A with ${}^R A^{\text{G}}$ and ${}^R A^{\text{E}}$, respectively, as in Eq. (5). Paralleling Eq. (4), the R asymptotic charge reads

$${}^R Q[\alpha] = \int_{\partial^R \Sigma} \alpha * F, \quad (14)$$

where ${}^R \Sigma$ is an R Cauchy surface. By Eq. (12),

$$\mathcal{Q} = {}^L Q + {}^R Q, \quad \mathcal{S} = {}^L S + {}^L S + {}^R S. \quad (15)$$

Entanglement. Let us now study how states in the Minkowski and Einstein Hilbert spaces embed into the product space of the L and R Milne patches. We start by showing that the common vacuum of the former is thermal with respect to the latter. After analyzing constraints on the soft modes, we evaluate their contribution to the entanglement between the L and R patches.

Relation between vacua. Weyl invariance of Maxwell theory allows us to prepare the vacuum state $|0\rangle$ of the Minkowski and Einstein spacetimes with a Euclidean path integral over an S^4 hemisphere. As described in the Appendix, the same path integral prepares an entangled thermal state from the Milne perspective. As a result, the vacuum state $|0\rangle$ is identified with a thermofield double state on L and R . An analogous path integral argument leads to the thermality of Rindler wedges and could alternatively be deduced from an analysis of the Bogoliubov transformations relating the Minkowski and Milne modes. In particular, demanding that $|0\rangle$ and the Milne vacua ${}^{L/R}|0\rangle$ be annihilated by the respective annihilation operators, one finds

$$|0\rangle \propto e^{-\mathcal{K}^+ L}|0\rangle^R|0\rangle, \quad (16)$$

where the entangling operator is given by

$$\mathcal{K}^+ = - \int_0^\infty d\lambda e^{-\pi\lambda} \int e^{(2)} (L\tilde{a}^{1+i\lambda})^\dagger \cdot ({}^R a^{1-i\lambda})^\dagger \quad (17)$$

in terms of Milne creation operators. Here, $e^{(2)}$ is the volume form over celestial space [27].

Turning to the soft modes, rather than relying on the $\lambda \rightarrow 0$ limit of our analysis above, we instead study the constraints [38] that entangle the edge modes [39,40] (see related results in [41,42]).

Soft constraints. In gauge theory, upon stitching together two complementary regions ${}^L \Sigma, {}^R \Sigma$ of a Cauchy slice, the physical Hilbert space \mathcal{H} is not simply the product of the L, R Hilbert spaces ${}^L \mathcal{H} \otimes {}^R \mathcal{H}$. Rather, the admissible physical states satisfy constraints [38].

For example, Gauss's law at the entangling surface $\partial^L \Sigma = -\partial^R \Sigma$ requires continuity of the normal component of the electric field [38], $\mathcal{Q}^{\text{ent}} \equiv {}^L Q + {}^R Q = 0$. The Hilbert space \mathcal{H} of the theory covering the full Cauchy surface is then the kernel $\mathcal{H} = \ker \mathcal{Q}^{\text{ent}} \subset {}^L \mathcal{H} \otimes {}^R \mathcal{H}$. This relates the Hilbert spaces of the Einstein universe and L, R Milne patches.

However, \mathcal{Q}^{ent} is precisely the asymptotic charge \mathcal{Q} in Eq. (15), which is nontrivial in the Minkowski Hilbert space. Instead, an appropriate constraint annihilating this Hilbert space can be selected by finding a linear combination of L, R soft operators that commutes with the Minkowski operators \mathcal{Q} and \mathcal{S} ,

$$\mathcal{Q}^{\text{ent}} = {}^L Q + {}^R Q + 2({}^L S - {}^R S). \quad (18)$$

The extra terms account for the sources in Fig. 2(b), which violate Gauss's law. Due to mixing with hard modes, \mathcal{Q}^{ent} in fact only annihilates the Minkowski Hilbert space in the $\epsilon \rightarrow 0$ limit, as discussed later.

Because the vacuum $|0\rangle$ is shared by the Einstein and Minkowski theories, it is annihilated by \mathcal{Q} and \mathcal{Q}^{ent} (with $\epsilon \rightarrow 0$). The Minkowski Hilbert space also contains states $|q\rangle$ with asymptotic charges $\mathcal{Q}[\alpha] = \int \epsilon^{(2)} q \alpha$ parametrized by a celestial scalar function $q(\mathbf{w})$ [43]. These $|q\rangle$ carry a background

$$A^{\text{CS}}[q] = \frac{1}{4\pi} \int \epsilon^{(2)}(\mathbf{w}) q(\mathbf{w}) A^{\text{CSI}}(\mathbf{w}, \infty), \quad (19)$$

produced by dressing [44]

$$|q\rangle = e^{i\mathcal{S}[q]}|0\rangle, \quad \mathcal{S}[q] = -i\langle A^{\text{CS}}[q], A \rangle. \quad (20)$$

Since $\mathcal{S}[q]$ is linear in A_a^{CS} , it is also linear in \mathcal{S}_a . Hence, it can be shown using Eq. (15) that $[\mathcal{S}[q], \mathcal{Q}^{\text{ent}}] = 0$, so $|q\rangle$ satisfies the Minkowski constraint.

Entanglement of edge modes. Let us now consider the R reduced density matrices of the states $|q\rangle$

$${}^R \rho[q] \equiv \text{tr}_{{}^L \mathcal{H}} |q\rangle \langle q| = e^{i{}^R \mathcal{S}[q]/2} {}^R \rho[0] e^{-i{}^R \mathcal{S}[q]/2}. \quad (21)$$

Hence, ${}^R \rho[q]$ and ${}^R \rho[0]$ are unitarily related because $\mathcal{S}[q] = \frac{1}{2} {}^R \mathcal{S}[q] + {}^L(\dots)$ [36]. Here, ${}^R \mathcal{S}[q]$ is defined in analogy to Eq. (20), using the R inner product with

$${}^R A^{\text{E}}[q] = \frac{1}{2\pi} \int \epsilon^{(2)}(\mathbf{w}) q(\mathbf{w}) {}^R A^{\text{EI}}(\mathbf{w}, \infty), \quad (22)$$

where ${}^R A^{\text{EI}}$ is constructed from ${}^R A^{\text{E}}$ in the same manner as Eq. (11). By design, ${}^R A^{\text{E}}[q]$ has Milne asymptotic charge ${}^R Q[\alpha] = \int \epsilon^{(2)} q \alpha$. Thus, all ${}^R \rho[q]$ share the same spectrum and von Neumann entropy (1), being merely dressed by different edge mode backgrounds.

Therefore, we focus on the entanglement of $|0\rangle$, which yields ${}^R \rho[0]$. Because

$$[{}^R\mathcal{Q}, {}^R\rho[0]] = -\text{tr}_{\mathcal{H}}[{}^L\mathcal{Q}, |0\rangle\langle 0|] = 0, \quad (23)$$

${}^R\rho[0]$ admits a decomposition into blocks ${}^R\rho[0, q]$ of definite ${}^R\mathcal{Q}$ (or equivalently RQ) [39,40]

$${}^R\rho[0] = \int \mathcal{E}[q] p[q] {}^R\rho[0, q],$$

$${}^R\mathcal{Q}[\alpha] {}^R\rho[0, q] = {}^R\rho[0, q] {}^R\mathcal{Q}[\alpha] = \left(\int \epsilon^{(2)} \alpha q \right) {}^R\rho[0, q], \quad (24)$$

where $\mathcal{E}[q]$ and $p[q]$ are a measure and probability distribution over the functions q . Further, $\text{tr} {}^R\rho[0, q] = 1$.

Isolating blocks ${}^R\rho[0, q]$ by fixing the Milne asymptotic charge in a path integral representation of ${}^R\rho[0]$, we find the blocks differ in their edge mode background (22), but share identical quantum fluctuations (due to the theory being free) [39,40]. This leads to the unitary relation [36]

$${}^R\rho[0, q] = e^{iRS[q]} {}^R\rho[0, 0] e^{-iRS[q]} = {}^R\rho[2q, 0]. \quad (25)$$

Consequently, the von Neumann entropy of Eq. (24) decomposes into two independent pieces [39,40]

$$S_{\text{vN}}({}^R\rho[0]) = S_{\text{Sh}}(p) + S_{\text{vN}}({}^R\rho[0, 0]), \quad (26)$$

where the Shannon entropy $S_{\text{Sh}}(p)$ of $p[q]$ is identified as the edge mode contribution [45]. In contrast to [39,40] the edge modes are identified with conformally soft modes (11). We demonstrate in [36] that these differ from the static modes in [39,40] by a gauge transformation.

Further, our path integral analysis identifies the factor $p[q] \propto \exp[-I_{2\pi}[{}^R A^E[q]]]$ due to the additive contribution made by the background shift (22) to the Euclidean action $I_{2\pi}$ [46]. Explicitly [47],

$$I_{\beta}[{}^R A^E[q]] = \frac{-\beta}{2 \log(\frac{1}{\epsilon})} \int \epsilon^{(2)} q (\square^{(2)})^{-1} q + \mathcal{O}(\log^{-2}(1/\epsilon)) \quad (27)$$

where $(\square^{(2)})^{-1}$ denotes convolution with the celestial Green's function [27]. The similarity to the edge mode action of [39,40], despite their focus on the spacetime interior, is natural from the Einstein universe perspective.

Discussion. Let us consider now the holographic interpretation of the entanglement studied in this Letter. Emulating Eq. (5) using the Milne modes (8) and inner products (9), we construct operators ${}^L\tilde{\mathcal{O}}_a^\Delta, {}^R\mathcal{O}_a^\Delta$. In the \cong sense, ${}^R\mathcal{O}_a^\Delta$ is proportional to annihilation and creation operators, ${}^R a_a^{1-i\lambda}(\mathbf{w})$, ${}^R a_a^{1+i\lambda}(\mathbf{w})^\dagger$, for $\Delta = 1 + i\lambda$ and $1 - i\lambda$ (with $\lambda > 0$), respectively. These appear in a mode expansion of the field operator, multiplying the positive and negative Milne frequency modes $({}^R A^{1+i\lambda})^a(\mathbf{w})$ and $({}^R A^{1-i\lambda})^a(\mathbf{w})$, respectively. Similarly, ${}^L\tilde{\mathcal{O}}_a^\Delta(\mathbf{w})$ is proportional to ${}^L\tilde{a}_a^{1+i\lambda}(\mathbf{w})$

and ${}^L\tilde{a}_a^{1+i\lambda}(\mathbf{w})^\dagger$. Holographically, ${}^L\tilde{\mathcal{O}}_a^\Delta, {}^R\mathcal{O}_a^\Delta$ are seen as conformal primaries in two sectors ${}^L\text{CFT}, {}^R\text{CFT}$ dual to the respective bulk Milne theories.

However, these sectors of the CCFT are not independent. To see this, we can express the entangling operator (A5) as a coupling between ${}^L\tilde{\mathcal{O}}^\Delta$ and ${}^R\mathcal{O}^\Delta$. For example, amplitudes in the $|0\rangle$ state are evaluated by CFT correlation functions in the presence of this interaction,

$$\langle 0 | \bullet | 0 \rangle = \langle e^{-\mathcal{K}^+ - (\mathcal{K}^+)^\dagger} \bullet \rangle_{{}^L\text{CFT}, {}^R\text{CFT}}. \quad (28)$$

With \bullet in ${}^R\text{CFT}$, the holographic dual of the thermal expectation value (A3) arises by tracing out ${}^L\text{CFT}$, i.e., $\langle e^{-{}^R\mathcal{K}} \bullet \rangle_{{}^R\text{CFT}}$ with

$${}^R\mathcal{K} = - \int_0^\infty \frac{d\lambda e^{-2\pi\lambda}}{(2\pi)^3} \frac{1 + \lambda^2}{2\lambda} \int \epsilon^{(2)R} \mathcal{O}^{1-i\lambda} \cdot {}^R\mathcal{O}^{1+i\lambda}. \quad (29)$$

Expanding the exponential in Eq. (29) yields a series of correlation functions weighted by $(e^{-2\pi\lambda})^n$ and the entanglement entropy corresponds to the von Neumann entropy of this distribution. This procedure is reminiscent of [48], which examines entanglement between two interacting CFT. However, their framework allows for a standard evaluation of entanglement entropy of the resulting mixed state, which is not the case for the CCFT.

Our calculations relied on the Maxwell theory being both free and Weyl invariant. So, what general lessons have been learned? Much of the analysis would carry through for a (weakly) interacting conformal gauge theory (e.g., $\mathcal{N} = 4$ super-Yang-Mills). However, one clear distinction arises since the unitary relation (25) fails. Hence, there is not a separation (26) between independent hard and soft contributions to the entanglement entropy. If Weyl invariance is also lost, e.g., by introducing massive particles, asymptotic states would still decompose in terms of modes with support to the future and past of the cut on \mathcal{I}^+ and the Minkowski vacuum $|0\rangle$ would be some entangled state of these modes. The decomposition would again divide the CCFT into two sectors interacting through the entangling operator.

While one sector would still correspond to the ${}^R\text{CFT}$ dual to the R patch, it is interesting to speculate on the organization of the remaining modes. Recall that the full Minkowski spacetime can be foliated with (Euclidean) AdS and dS slices [49–53], as in Fig. 1(a). One might conjecture that the P, Q, R patches have their own dual CFTs that mutually interact to exchange excitations and encode entanglement in spacetime. It would be interesting to explore these speculations further.

Further details can be found in [36]. There, we evaluate the edge mode partition function [39,40], from which $S_{\text{Sh}}(p)$ is easily computed. We also draw connections to the CFT renormalization and cutoff scales.

Acknowledgments. We would like to thank Freddy Cachazo, Laurent Freidel, and especially Sabrina Pasterski for helpful discussions. Research at Perimeter Institute is supported in part by the Government of Canada through the Department of Innovation, Science, and Economic Development Canada and by the Province of Ontario through the Ministry of Colleges and Universities. H. Z. C. and R. C. M. were also supported by the Natural Sciences and Engineering Research Council of Canada. R. C. M. was also supported by funding from the BMO Financial Group and the Simons Foundation “It from Qubit” collaboration. A. R. is supported by the Heising-Simons Foundation “Observational Signatures of Quantum Gravity” collaboration Grant No. 2021-2817 and acknowledges Perimeter Institute for hospitality while this work has been completed.

Appendix: Entanglement from path integrals. Weyl invariance of Maxwell theory allows us to prepare the vacuum state $|0\rangle$ of the Minkowski and Einstein spacetimes with a Euclidean path integral over an S^4 hemisphere, as shown in Fig. 4(a). However, the same path integral prepares an entangled thermal state from the Milne perspective—see Fig. 4(b). That is, the overlap ${}^L\langle\varphi'|{}^R\langle\varphi|0\rangle$ with L, R states coincides with the matrix element of an evolution by π in imaginary Milne time τ ,

$${}^L\langle\varphi'|{}^R\langle\varphi|0\rangle \propto {}^R\langle\varphi|e^{-\pi^R H R}|\tilde{\varphi}'\rangle \quad (\text{A1})$$

$$\Rightarrow |0\rangle \propto \sum_i e^{-\pi E_i L} |\tilde{E}_i\rangle^R |E_i\rangle, \quad (\text{A2})$$

where ${}^R H$ is the R Hamiltonian, with eigenstates ${}^R |E_i\rangle$ and eigenvalues E_i . A CPT transformation in Eq. (A1) reinterprets the path integral boundary condition set by the L state ${}^L\langle\varphi'|$ as an R state ${}^R|\tilde{\varphi}'\rangle$ —for Maxwell theory, this coincides with the shadow transformation. Hence, $|0\rangle$ is a thermofield double state on L and R , and tracing over the L Hilbert space yields the thermal state

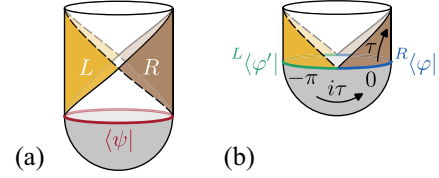


FIG. 4. (a) The common Einstein and Minkowski vacuum is prepared by a Euclidean path integral over an S^4 hemisphere. (b) The same path integral prepares an L, R thermofield double.

$${}^R\rho[0] \equiv \text{tr}_{{}^L\mathcal{H}}|0\rangle\langle 0| \propto e^{-2\pi^R H}. \quad (\text{A3})$$

This closely parallels the path integral argument for the thermality of Rindler wedges and, in fact, the L, R Milne patches can be conformally mapped to Rindler wedges.

As in the Rindler case, Eq. (A2) may alternatively be deduced by studying mode decompositions. With $\Delta = 1 + i\lambda$, Eq. (8) coincides precisely with the Unruh [54] construction of positive- and negative-definite Minkowski frequency modes in terms of L, R modes with frequency λ . Thus, the resulting Bogoliubov transformations relating Minkowski and Milne annihilation operators are identical to the Rindler case. Demanding $|0\rangle$ and the Milne vacua ${}^{L/R}|0\rangle$ be annihilated by the respective annihilation operators, one finds

$$|0\rangle \propto e^{-\mathcal{K}^+ L} |0\rangle^R |0\rangle, \quad (\text{A4})$$

where the entangling operator is given by

$$\mathcal{K}^+ = - \int_0^\infty d\lambda e^{-\pi\lambda} \int e^{(2)} ({}^L \tilde{a}^{1+i\lambda})^\dagger \cdot ({}^R a^{1-i\lambda})^\dagger \quad (\text{A5})$$

in terms of Milne creation operators. Here, $e^{(2)}$ is the volume form over celestial space [27]. Since each Milne creation operator increments the Milne energy E by λ , we have recovered Eq. (A2).

[1] J. M. Maldacena, *Adv. Theor. Math. Phys.* **2**, 231 (1998).
[2] S. Ryu and T. Takayanagi, *J. High Energy Phys.* **08** (2006) 045.
[3] S. Ryu and T. Takayanagi, *Phys. Rev. Lett.* **96**, 181602 (2006).
[4] A. Lewkowycz and J. Maldacena, *J. High Energy Phys.* **08** (2013) 090.
[5] T. Faulkner, A. Lewkowycz, and J. Maldacena, *J. High Energy Phys.* **11** (2013) 074.
[6] M. Rangamani and T. Takayanagi, *Lect. Notes Phys.* **931**, 1 (2017).

[7] A. Almheiri, X. Dong, and D. Harlow, *J. High Energy Phys.* **04** (2015) 163.
[8] F. Pastawski, B. Yoshida, D. Harlow, and J. Preskill, *J. High Energy Phys.* **06** (2015) 149.
[9] A. Almheiri, N. Engelhardt, D. Marolf, and H. Maxfield, *J. High Energy Phys.* **12** (2019) 063.
[10] G. Penington, *J. High Energy Phys.* **09** (2020) 002.
[11] A. Almheiri, R. Mahajan, J. Maldacena, and Y. Zhao, *J. High Energy Phys.* **03** (2020) 149.
[12] A. Strominger, *J. High Energy Phys.* **07** (2014) 151.
[13] A. Strominger, *J. High Energy Phys.* **07** (2014) 152.

- [14] T. He, V. Lysov, P. Mitra, and A. Strominger, *J. High Energy Phys.* **05** (2015) 151.
- [15] T. He, P. Mitra, A. P. Porfyriadis, and A. Strominger, *J. High Energy Phys.* **10** (2014) 112.
- [16] D. Kapec, V. Lysov, S. Pasterski, and A. Strominger, *J. High Energy Phys.* **08** (2014) 058.
- [17] T. He, P. Mitra, and A. Strominger, *J. High Energy Phys.* **10** (2016) 137.
- [18] A. Strominger, *Lectures on the Infrared Structure of Gravity and Gauge Theory* (Princeton University Press, Princeton, NJ, 2018).
- [19] A.-M. Raclariu, arXiv:2107.02075.
- [20] S. Pasterski, *Eur. Phys. J. C* **81**, 1062 (2021).
- [21] D. Kapec, A.-M. Raclariu, and A. Strominger, *Classical Quantum Gravity* **34**, 165007 (2017).
- [22] E. P. Verlinde and K. M. Zurek, *Phys. Lett. B* **822**, 136663 (2021).
- [23] K. M. Zurek, *Phys. Lett. B* **826**, 136910 (2022).
- [24] E. Verlinde and K. M. Zurek, *Phys. Rev. D* **106**, 106011 (2022).
- [25] S. Pasterski and S.-H. Shao, *Phys. Rev. D* **96**, 065022 (2017).
- [26] S. Pasterski and A. Puhm, *Phys. Rev. D* **104**, 086020 (2021).
- [27] See Supplemental Material at <http://link.aps.org/supplemental/10.1103/PhysRevD.109.L121702> for a summary of our conventions.
- [28] L. Donnay, A. Puhm, and A. Strominger, *J. High Energy Phys.* **01** (2019) 184.
- [29] Asymptotic charge conservation states that Eq. (4) is independent of the choice of \pm .
- [30] G. R. Brown, J. Gowdy, and B. Spence, *Phys. Rev. D* **108**, 066009 (2023).
- [31] E. Jørstad, S. Pasterski, and A. Sharma, *J. High Energy Phys.* **02** (2024) 228.
- [32] S. W. Hawking and G. F. R. Ellis, *The Large Scale Structure of Space-Time* (Cambridge University Press, Cambridge, England, 1973).
- [33] L. Donnay, S. Pasterski, and A. Puhm, *J. High Energy Phys.* **09** (2020) 176.
- [34] D. Kapec, M. Perry, A.-M. Raclariu, and A. Strominger, *Phys. Rev. D* **96**, 085002 (2017).
- [35] One may also consider timelike sources passing through t^0 , contributing additionally to Q^\pm through an H_3 bulk-to-boundary propagator.
- [36] H. Z. Chen, R. Myers, and A.-M. Raclariu, arXiv:2403.13913.
- [37] G. Satishchandran and R. M. Wald, *Phys. Rev. D* **99**, 084007 (2019).
- [38] W. Donnelly and L. Freidel, *J. High Energy Phys.* **09** (2016) 102.
- [39] W. Donnelly and A. C. Wall, *Phys. Rev. D* **94**, 104053 (2016).
- [40] W. Donnelly and A. C. Wall, *Phys. Rev. Lett.* **114**, 111603 (2015).
- [41] K. W. Huang, *Phys. Rev. D* **92**, 025010 (2015).
- [42] A. Ball, A. Law, and G. Wong, arXiv:2403.14542.
- [43] The mean of q is required to vanish, corresponding to a vanishing global charge.
- [44] N. Arkani-Hamed, M. Pate, A.-M. Raclariu, and A. Strominger, *J. High Energy Phys.* **08** (2021) 062.
- [45] Rényi entropies decompose similarly.
- [46] ${}^R\rho[0]$ is prepared with two copies of the Euclidean path integral in Fig. 4(b), extending the range of $i\tau$ to 2π .
- [47] In Eq. (27), we have switched to a different ϵ regulator from that inherited from A^{CS} in Eq. (12). Following [39,40], ${}^R A^{\text{E}}$ is defined to be an *exactly* Milne-static solution with electric field lines penetrating $\partial^R\Sigma$ as shown in Fig. 3, except now $\partial^R\Sigma$ is placed at a cutoff e^2 in the Fefferman-Graham coordinate $\rho = 2u/r$ along the Euclidean AdS ${}^R\Sigma$. When $\epsilon \rightarrow 0$, the electric field lines bunch up to $\rho = e^2 \rightarrow 0$, similar to Fig. 3. This static ${}^R A^{\text{E}}$ agrees with A^{log} (with the old ϵ removed) in R up to rescaling and a gauge transformation [36].
- [48] A. Mollabashi, N. Shiba, and T. Takayanagi, *J. High Energy Phys.* **04** (2014) 185.
- [49] J. de Boer and S. N. Solodukhin, *Nucl. Phys.* **B665**, 545 (2003).
- [50] C. Cheung, A. de la Fuente, and R. Sundrum, *J. High Energy Phys.* **01** (2017) 112.
- [51] N. Ogawa, T. Takayanagi, T. Tsuda, and T. Waki, *Phys. Rev. D* **107**, 026001 (2023).
- [52] L. Iacobacci, C. Sleight, and M. Taronna, *J. High Energy Phys.* **06** (2023) 053.
- [53] C. Sleight and M. Taronna, arXiv:2301.01810.
- [54] W. G. Unruh, *Phys. Rev. D* **14**, 870 (1976).